Biomolecular screening with encoded porous-silicon photonic crystals

FRÉDÉRIQUE CUNIN[1], THOMAS A. SCHMEDAKE[1], JAMIE R. LINK[1], YANG YANG LI[1] JENNIFER KOH[2], SANGEETA N. BHATIA[2] AND MICHAEL J. SAILOR*[1]

[1]Department of Chemistry and Biochemistry, University of California, San Diego, 9500 Gilman Drive, Department 0358, La Jolla, California 92093-0358, USA
[2]Department of Bioengineering, University of California, San Diego, 9500 Gilman Drive, Department 0412, La Jolla, California 92093-0412, USA
*e-mail: msailor@ucsd.edu

Published online: 2 September 2002; doi:10.1038/nmat702

Strategies to encode or label small particles or beads for use in high-throughput screening and bioassay applications[1] focus on either spatially differentiated, on-chip arrays[2–4] or random distributions of encoded beads[5,6]. Attempts to encode large numbers of polymeric, metallic or glass beads in random arrays or in fluid suspension have used a variety of entities to provide coded elements (bits)—fluorescent molecules, molecules with specific vibrational signatures[7,8], quantum dots[9], or discrete metallic layers[10]. Here we report a method for optically encoding micrometre-sized nanostructured particles of porous silicon. We generate multilayered porous films in crystalline silicon using a periodic electrochemical etch. This results in photonic crystals with well-resolved and narrow optical reflectivity features, whose wavelengths are determined by the etching parameters[11]. Millions of possible codes can be prepared this way. Micrometre-sized particles are then produced by ultrasonic fracture[12], mechanical grinding or by lithographic means. A simple antibody-based bioassay using fluorescently tagged proteins demonstrates the encoding strategy in biologically relevant media.

We prepared encoded particles by a galvanostatic anodic etch of crystalline silicon wafers. The electrochemical process generates an optically uniform layer of porous silicon: the thickness and porosity of a given layer is controlled by the current density, the duration of the etch cycle, and the composition of the etchant solution[11,13]. Photonic structures approximating rugate filters[14] (multilayered stacks in which the refractive index varies sinusoidally, resulting in a mirror with high reflectivity in a narrow spectral region) were prepared by applying a computer-generated pseudo-sinusoidal current waveform to the etch cell, following previously published procedures[11,14–22]. The resulting multilayers were removed from the substrate using a current pulse, and mechanically agitated or ultrasonicated[12] to create particles. By masking the wafer before etching, well-defined slabs of particles can be generated (Fig. 1). The multilayered photonic crystals generated in this fashion display a very sharp line in the optical reflectivity spectrum; this line can appear anywhere in the visible to near-infrared spectral range, depending on the waveform used in the programmed etch (Fig. 2). These spectral features can be much narrower than the fluorescence spectrum obtained from a molecule or core-shell quantum dot. For example, the spectral band of the single-mode rugate filter shown in Fig. 3 has a full-width at half-maximum (FWHM) of 11 nm, whereas the narrowest quantum dot spectrum reported at this

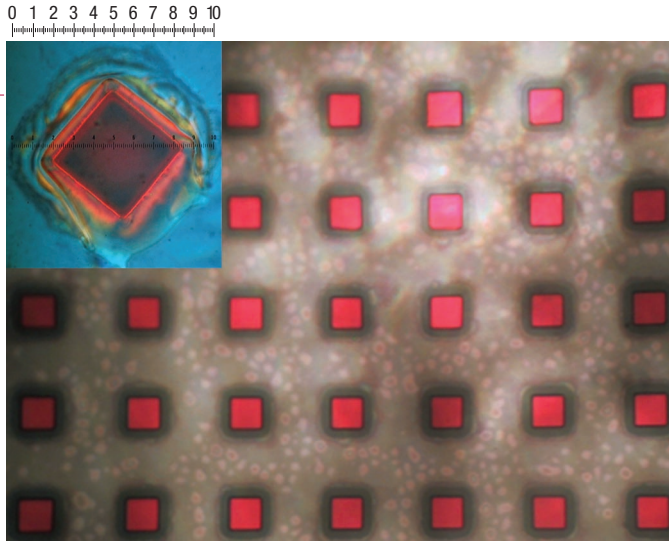

Figure 1 Optical microscope image of rugate-encoded porous-silicon particles photolithographically defined into 94-mm squares, 5 mm thick, on a silicon wafer. Inset, a square particle after removal from the substrate (see Methods). The colour of the particles derives from the periodicity defined in the photonic crystal during the etch. These samples were prepared to display a photonic spectral maximum at 632 nm. The scale in the inset (reproduced above the figure for clarity) corresponds to 2 μm per small division.

wavelength has a FWHM of 20 nm (ref. 1). Multiple rugate structures can be etched on a single particle (Fig. 3) and even in the same physical location[14], showing that many sharp spectral lines (code elements, or bits) can be obtained on a single micrometre-sized particle.

In order to test the reliability of the encoding approach in a biological screening application, we prepared two different batches of encoded particles as single rugate structures. Both batches of particles were ozone-oxidized to improve their stability in aqueous media and to provide a hydrophilic surface. Particles coded with a 750-nm spectral feature were then treated with a concentrated solution of bovine serum albumin (BSA) and incubated for three hours. This batch of particles served as the control. In a separate Petri dish, 540-nm-encoded particles were exposed to 50 μg ml^{-1} rat albumin in buffer, and incubated for two hours. This operation resulted in a specific modification of the surface of the

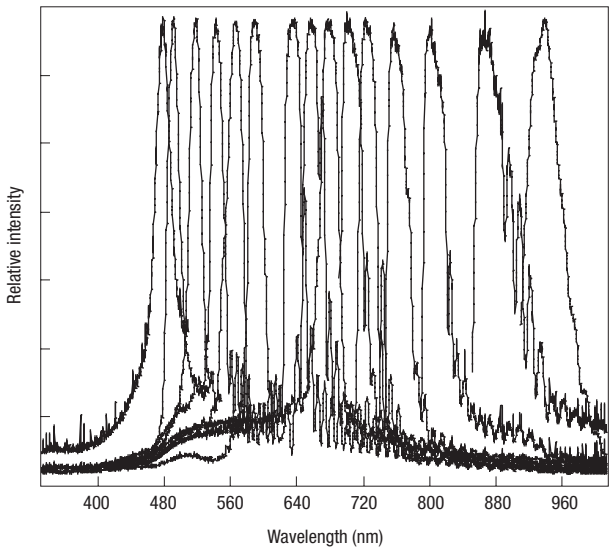

Figure 2 Reflectivity spectra of 15 porous-silicon multilayered samples prepared using a sinusoidal etch (rugate photonic structure); see Methods for details. Each of the samples contains a single rugate frequency code. Spectra were obtained using a Cambridge Instruments microscope with a 70× objective. The sample was illuminated using a tungsten lamp, and the reflected light spectrum was measured with an Ocean Optics SD2000 CCD (charge-coupled device) spectrometer.

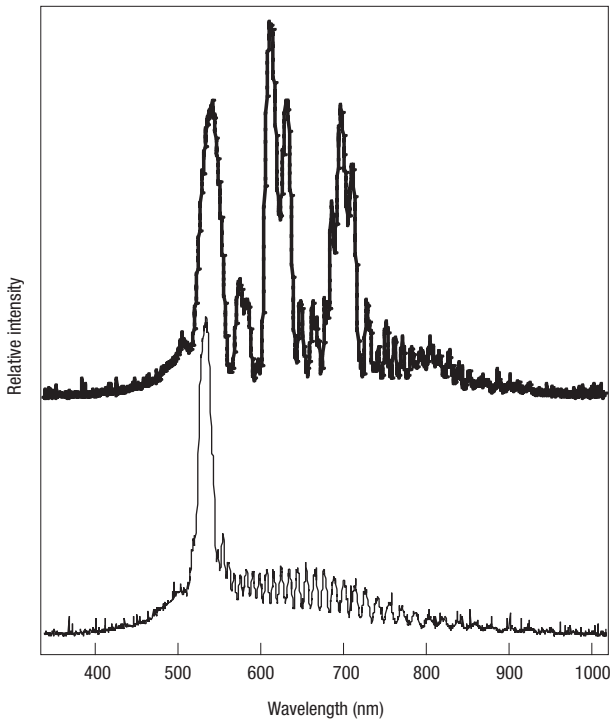

Figure 3 Reflectivity spectra of porous silicon rugate particles etched with a single periodicity (bottom) and with three separate periodicities (top). The particles display peaks in the spectrum characteristic of their multilayered structures. The sample represented in the bottom spectrum was etched using a sinusoidal current variation between 11.5 and 19.2 mA cm^{-2} with 50 repeats and a periodicity of 18 s. The triply encoded particle (triple rugate) represented by the top spectrum was prepared using a sinusoidal current variation oscillating between 11.5 and 34.6 mA cm^{-2} with a periodicity of 10 s for 20 periods (520 nm), 12 s for 45 periods (610 nm), and 14 s for 90 periods (700 nm). The approximate thickness of this sample is 15 μm. Spectra are offset along the *y* axis for clarity.

particles by direct adsorption of the protein. The rat-albumin-modified particles were then exposed to a primary rabbit anti-rat-albumin antibody in a concentrated solution of BSA, and incubated for one hour to obtain a specific antibody–antigen interaction. Both batches of particles were then mixed together and incubated for one hour in the presence of FITC- (fluorescein isothiocyanate) conjugated goat anti-rabbit immunoglobulin-G in a BSA solution. Detection of analyte binding to the encoded particles was then performed by fluorescence and spectral reflectance microscopy (Fig. 4).

Decoding, performed on 16 particles, yielded the following results: among eight green fluorescent particles, eight particles were positively decoded as belonging to the functionalized rat albumin batch (Fig. 4a). Among the eight non-luminescent particles, six particles were correctly decoded (Fig. 4b), one particle displayed the incorrect code and one particle was unreadable. Presumably the particle that displayed the incorrect code belonged to the first batch but was not sufficiently functionalized with rat albumin to generate fluorescence in the antibody assay. This is understandable, because in the present study the rat albumin was not covalently attached to the silica-coated particles. A variety of stable chemical modification chemistries have been developed for oxidized and non-oxidized porous silicon, and some of these have been demonstrated with specific antibodies or receptors[23–26]. Thus the issue of immobilizing biochemical or chemical components is not expected to be significant. Additionally, chemical modification can prevent corrosion in aqueous media[27], which may otherwise lead to undesirable shifts in the optical code and/or unreadable particles. In the current study, no passivating chemical treatments, other than ozone oxidation to generate a layer of silica, were performed, and upon immersion in basic aqueous media the spectral codes were observed to shift between 0 and 50 nm depending on the incubation times.

The layered porous-silicon photonic structures offer several advantages over existing encoding methodologies. Porous-silicon photonic structures can be constructed that display features spanning the visible, near-infrared and infrared regions of the spectrum[11]. The present work represents, to our knowledge, the first example of a single material that can be used to encode over such a broad wavelength range. For a given semiconductor type, quantum dots have a more limited spectral range in which they emit. In addition, the reflectance spectra of rugate filters can exhibit much sharper spectral features than can be obtained from a gaussian ensemble of quantum dots. Thus more codes can be placed in a narrower spectral window with the photonic structures. Unlike encoding schemes based on stratified metallic nanorods[10], fluorescence or vibrational signatures[7,8], photonic crystals can be probed using light diffraction techniques[28]; thus it is not necessary to use imaging optics in order to read the codes. In the present work the encoded particles were assayed using a conventional fluorescence tagging technique, although previous work has established that sensitive chemical and biochemical detection can be built into the optical structure of photonic crystals[20,25], eliminating the need for fluorescent probes and focusing optics[28]. In addition, because the oxidized porous-silicon particles present a silica-like surface to the environment, they do not readily quench luminescence from organic chromophores, and they can be handled and modified using the chemistries developed for glass bead bioassays[29]. The fact that the materials are silicon-based means that they can be readily integrated with existing chip technologies.

The use of encoded silicon nanostructures in medical diagnostic applications has advantages over organic dyes or quantum dots. *In vivo* studies have shown the biocompatibility of porous silicon, as well as the long-term stability of reflectance data from multilayer structures[27]. Recent work has demonstrated the biocompatibility of overcoated CdSe quantum dots[30], but there are still unresolved issues involving the

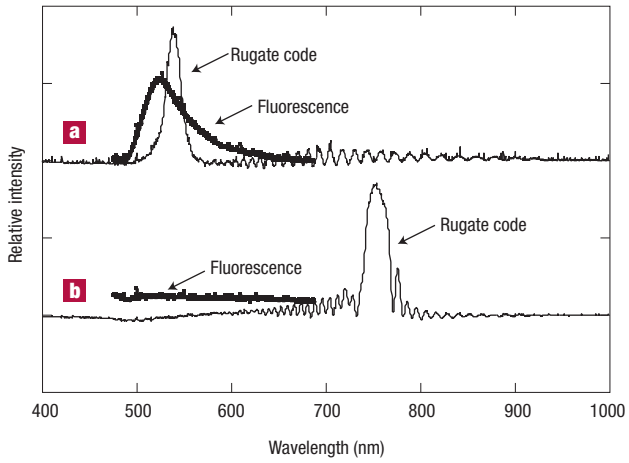

Figure 4 Fluorescence and optical reflectivity spectra (background correction applied) for two rugate-encoded particles. a, Particles functionalized with rat albumin, then assayed with the FITC-conjugated secondary antibody. **b**, Control particles treated with bovine serum albumin and assayed with the FITC-conjugated anti-rat secondary antibody. Particles were etched using a sinusoidal current varying between 11.5 and 34.6 mA cm^{-2} with 70 repeats and a periodicity of **a**, 10 s (λ = 540 nm) and **b**, 14 s (λ = 750 nm); approximate rugate unit cell dimension is 180 nm and 250 nm, respectively. The particles used in this experiment were of the order of 100 μm in diameter and 10 μm thick. Fluorescence measurements were obtained using a Nikon dark-field microscope with a 5× objective, coupled to a Spex 270M spectrometer and Princeton Instruments CCD detector with an exposure time of 60 s. Spectral regions were selected using a 2-mm image plane aperture, resulting in a 200-μm sample size. Spectra are offset along the *y* axis for clarity.

incorporation of potentially toxic heavy metals into living systems. Additionally, the possibility of optically addressing particles at near-infrared, tissue-penetrating wavelengths without the losses associated with low fluorescence quantum yields makes these materials amenable to *in vivo* diagnostics. Finally, because the rugate filters are an integral and orderly part of the porous structure, it is not possible for part of the code to be lost, scrambled or photobleached, as can occur with quantum dots or fluorescent molecules.

METHODS

SAMPLE PREPARATION

Porous silicon samples were prepared by anodically etching p^{++} type, B-doped, (100)-oriented silicon with resistivity <1 mΩ cm (Siltronix, Inc.) in a solution of 48% aqueous HF:ethanol (3:1 by volume). Typical etch parameters for a rugate structure involved a pseudosinusoidal current waveform oscillating between 11.5 and 19.2 mA cm^{-2} with 50 repeats and a periodicity of 18 s. Films were removed from the substrate using a current pulse of 460 mA cm^{-2} for 40 s. Lithographically defined particles were prepared by applying an S-1813 photoresist (Shipley) to the wafer before the electrochemical etch (spin-coated at 4,000 r.p.m. for 60 s, soft-baked at 90 °C for 2 min, ultraviolet-exposed using a contact mask aligner, hard-baked at 120 °C for 30 min before development).

BIOASSAY

The two different classes (test and control) of encoded particles were oxidized in a stream of O_3 (Ozone Generator Model T12, TriO3 Industries, Inc., diluted with compressed air at 10 l min^{-1}) for 20 min. Control particles coded with a 750-nm spectral feature were treated with concentrated BSA (Sigma, 5 g in 100 ml of double-distilled water) and incubated at 37 °C under 5% CO_2 in air for three hours. The 540-nm-encoded test particles were exposed to 50 μg ml^{-1} rat albumin in coating buffer (2.93 g $NaHCO_3$, 1.61 g Na_2CO_3 in 1,000 ml double-distilled water), and incubated at 37 °C under 5% CO_2 for two hours. The test particles were then exposed to a 1:100 dilution of primary rabbit anti-rat-albumin antibody in a concentrated solution of BSA at 37 °C under 5% CO_2 for one hour. Both batches of particles were then mixed together and incubated for one hour in the presence of FITC-conjugated secondary antibody (goat anti-rabbit immunoglobulin-G, Sigma) in a BSA solution. After each step, a rinsing cycle with Dulbecco's phosphate buffered saline (PBS, Life Technologies) and with distilled water was performed.

Received 15 April 2002; accepted 1 July 2002; published 2 September 2002.

References

1. Bruchez, M., Moronne, M., Gin, P., Weiss, S. & Alivisatos, A. P. Semiconductor nanocrystals as fluorescent biological labels. *Science* **281,** 2013–2016 (1998).
2. Harrison, D. J. *et al.* Micromachining a miniaturized capillary electrophoresis-based chemical analysis system on a chip. *Science* **261,** 895–897 (1993).
3. Heller, M. J. An active microelectronics device for multiplex DNA analysis. *IEEE Eng. Med. Biol.* **15,** 100–104 (1996).
4. Chee, M. *et al.* Accessing genetic information with high-density DNA arrays. *Science* **274,** 610–614 (1996).
5. Still, W. C. Discovery of sequence-selective peptide binding by synthetic receptors using encoded combinatorial libraries. *Acc. Chem. Res.* **29,** 155–163 (1996).
6. Ferguson, J. A., Boles, T. C., Adams, C. P. & Walt, D. R. A fiber-optic DNA biosensor microarray for the analysis of gene expression. *Nature Biotechnol.* **14,** 1681–1684 (1996).
7. Fenniri, H., Ding, L., Ribbe, A. E. & Zyrianov, Y. Barcoded resins: a new concept for polymer-supported combinatorial library self-deconvolution. *J. Am. Chem. Soc.* **123,** 8151–8152 (2001).
8. Fenniri, H. *et al.* Towards the DRED of resin-supported combinatorial libraries: a non-invasive methodology based on bead self-encoding and multispectral imaging. *Angew. Chem. Int. Edn Engl.* **39,** 4483–4485 (2000).
9. Chan, W. C. W. & Nie, S. Quantum dot bioconjugates for ultrasensitive nonisotopic detection. *Science* **281,** 2016–2018 (1998).
10. Nicewarner-Peña, S. R. *et al.* Submicrometer metallic barcodes. *Science* **294,** 137–141 (2001).
11. Thonissen, M. & Berger, M. G. in *Properties of Porous Silicon* Vol. 18. (ed. Canham, L.) 30–37 (Short Run, London, 1997).
12. Heinrich, J. L., Curtis, C. L., Credo, G. M., Kavanagh, K. L. & Sailor, M. J. Luminescent colloidal Si suspensions from porous Si. *Science* **255,** 66–68 (1992).
13. Halimaoui, A. in *Properties of Porous Silicon* Vol. 18 (ed. Canham, L.) 12–22 (Short Run, London, 1997).
14. Berger, M. G. *et al.* Dielectric filters made of porous silicon: advanced performance by oxidation and new layer structures. *Thin Solid Films* **297,** 237–240 (1997).
15. Cazzanelli, M., Vinegoni, C. & Pavesi, L. Temperature dependence of the photoluminescence of all-porous-silicon optical microcavities. *J. Appl. Phys.* **85,** 1760–1764 (1999).
16. Lehmann, V., Stengl, R., Reisinger, H., Detemple, R. & Theiss, W. Optical shortpass filters based on macroporous silicon. *Appl. Phys. Lett.* **78,** 589–591 (2001).
17. Mazzoleni, C. & Pavesi, L. Application to optical components of dielectric porous silicon multilayers. *Appl. Phys. Lett.* **67,** 2983–2985 (1995).
18. Pavesi, L. & Dubos, P. Random porous silicon multilayers: application to distributed Bragg reflectors and interferential Fabry-Perot filters. *Semicond. Sci. Tech.* **12,** 570–575 (1997).
19. Pellegrini, V., Tredicucci, A., Mazzoleni, C. & Pavesi, L. Enhanced optical properties in porous silicon microcavities. *Phys. Rev. B* **52,** R14328–R14331 (1995).
20. Snow, P. A., Squire, E. K., Russell, P. S. J. & Canham, L. T. Vapor sensing using the optical properties of porous silicon Bragg mirrors. *J. Appl. Phys.* **86,** 1781–1784 (1999).
21. Vincent, G. Optical properties of porous silicon superlattices. *Appl. Phys. Lett.* **64,** 2367–2369 (1994).
22. Zangooie, S., Schubert, M., Trimble, C., Thompson, D. W. & Woollam, J. A. Infrared ellipsometry characterization of porous silicon Bragg reflectors. *Appl. Opt.* **40,** 906–912 (2001).
23. Dancil, K.-P. S., Greiner, D. P. & Sailor, M. J. A porous silicon optical biosensor: detection of reversible binding of IgG to a protein A-modified surface. *J. Am. Chem. Soc.* **121,** 7925–7930 (1999).
24. Tinsley-Bown, A. M. *et al.* Tuning the pore size and surface chemistry of porous silicon for immunoassays. *Phys. Status Solidi A* **182,** 547–553 (2000).
25. Chan, S., Horner, S. R., Miller, B. L. & Fauchet, P. M. Identification of gram negative bacteria using nanoscale silicon microcavities. *J. Am. Chem. Soc.* **123,** 11797–11798 (2001).
26. Starodub, N. F., Fedorenko, L. L., Starodub, V. M., Dikij, S. P. & Svechnikov, S. V. Use of the silicon crystals photoluminescence to control immunocomplex formation. *Sens. Actuators B* **35,** 44–47 (1996).
27. Canham, L. T. *et al.* Derivatized porous silicon mirrors: implantable optical components with slow resorbability. *Phys. Status Solidi A* **182,** 521–525 (2000).
28. Reese, C. E., Baltusavich, M. E., Keim, J. P. & Asher, S. A. Development of an intelligent polymerized crystalline colloidal array colorimetric reagent. *Anal. Chem.* **73,** 5038–5042 (2001).
29. Hermanson, G. T. *Bioconjugate Techniques* (Academic, San Diego, 1996).
30. Gerion, D. *et al.* Synthesis and properties of biocompatible water-soluble silica-coated CdSe/ZnS semiconductor quantum dots. *J. Phys. Chem. B* **105,** 8861–8871 (2001).

Acknowledgements

We thank E. Ruoslahti and T. Mustelin for discussions. This work was supported by the David and Lucile Packard Foundation, the National Science Foundation and the National Institute of Health. Correspondence and requests for materials should be addressed to M.J.S.

Competing financial interests

The authors declare that they have no competing financial interests.